The accuracies of effective interactions in downfolding coupled-cluster approaches for small-dimensionality active spaces

Karol Kowalski,[a] Bo Peng, and Nicholas P. Bauman

AFFILIATIONS

Physical Sciences Division, Pacific Northwest National Laboratory, Richland, Washington 99354, USA

[a]**Author to whom correspondence should be addressed:** karol.kowalski@pnnl.gov

ABSTRACT

This paper evaluates the accuracy of the Hermitian form of the downfolding procedure using the double unitary coupled cluster (DUCC) ansatz on the benchmark systems of linear chains of hydrogen atoms, H6 and H8. The computational infrastructure employs the occupation-number-representation codes to construct the matrix representation of arbitrary second-quantized operators, allowing for the exact representation of exponentials of various operators. The tests demonstrate that external amplitudes from standard single-reference coupled cluster methods that sufficiently describe external (out-of-active-space) correlations reliably parameterize the Hermitian downfolded effective Hamiltonians in the DUCC formalism. The results show that this approach can overcome the problems associated with losing the variational character of corresponding energies in the corresponding SR-CC theories.

I. INTRODUCTION

Applying many-body methods for dimensionality/cost reduction (DCR) of *ab initio* formulations is imperative in expanding the range of system sizes amenable to accurate many-body formulations in chemistry and material sciences. These techniques play a vital role in embracing new computational paradigms associated with the emergence of quantum computing and machine learning (ML) techniques. Accurate and rigorous DCR techniques are also critically needed to drive the design of new approaches capable of capturing the sparsity inherent to broad classes of correlated quantum systems. For example, these formalisms are instrumental in effectively using early quantum computing resources, commonly referred to as the noisy intermediate-scale quantum (NISQ) devices,[1–4] where DCR methods primarily focus on minimizing the number of qubits required to represent a given quantum problem. One should mention several techniques developed to take full advantage of the ubiquitous Variational Quantum Eigensolver (VQE) approach[5–16] in addressing problems beyond the situation where few electrons are correlated.

In the context of quantum chemistry, the utilization of DCR techniques is linked to the partitioning of electron correlation effects into static and dynamic partitions and capturing them in the many-body effective Hamiltonians acting in active spaces. The coupled cluster (CC) formalism[17–25] has been found to be particularly effective in capturing and separating the various effects. It provides a natural means of expressing effective Hamiltonians in terms of many-body correlation effects. The CC-driven DCR techniques can provide a mathematically rigorous platform for a broad utilization of deep neural networks (DNNs)[26–31] to learn the form of effective interactions in the small-dimensionality spaces, opening in this way prospects of performing affordable high-accuracy/interaction-driven simulations of chemical systems as envisioned in Refs. 32 and 33.

We have recently introduced and tested downfolding techniques based on the double unitary coupled cluster (DUCC)[34] ansatz to address the above-mentioned problems. This formalism falls into a broad class of unitary wave function ansatzen for describing the ground states of correlated systems.[35–45] The downfolding procedure utilizes the properties of the ground-state DUCC ansatz, which, in analogy to single-reference sub-system embedding sub-algebras (SES-CC),[46–48] allows us to construct effective Hamiltonians that integrate out-of-active-space degrees of freedom usually identified with dynamical correlation effects. In contrast to the SES-CC

approach, the DUCC formalism yields the Hermitian form of the effective Hamiltonian in the active space.

The DUCC-driven downfolded Hamiltonians and other CC-based downfolding techniques, such as the driven similarity renormalization group or active-space embedding theory,[4,49] are natural theoretical frameworks for the development of various CC-based embedding schemes. Recently, several approximations have been tested to validate the efficiency of the downfolding procedure. These approximations, due to the non-commutativity of the components defining DUCC operators, were based on (1) the maximum rank of the commutator expansions, (2) the limited rank of interactions included in the downfolded Hamiltonians (one- and two-body interactions), and (3) the choice of the approximate form of the external amplitudes [usually extracted from the single-reference CC (SR-CC) model with singles and doubles (CCSD)].[23] The DUCC-based techniques are also integral parts of the distributed algorithms based on the quantum flow approaches,[47,50] which can increase the system size limit that is tractable by NISQ devices and pave the road for novel formulations that capture the general-type sparsity of correlated quantum systems.

Our team has recently developed a novel full configuration interaction (FCI) code called stringMB,[48] which employs a string-based approach to emulate quantum systems and represent operators in matrix form. This code has been integrated into the NWChem software, enabling us to (1) work with the exact representations of operator exponents and (2) leverage various sources for external CC amplitudes. This allows us to focus strictly on the role of SR-CC amplitudes by removing the ambiguity of the other approximations as we include the exact representation of the operator exponentials and all many-body ranks of interactions. In this study, we investigate the impact of higher-rank external excitations obtained through CCSD,[23] CCSDT,[51–53] and CCSDTQ[54–56] simulations, as well as the active space size, on the accuracy of ground-state energies for small benchmark systems H6 and H8 representing linear chains of hydrogen atoms.

II. THEORY

The DUCC formulations have been amply discussed in recent papers (see Refs. 32–34). Here, we overview only the salient features of these approaches. While the SES-CC technique[46,47] forms the basis for non-Hermitian downfolding, the DUCC expansions provide its Hermitian formulations. The Hermitian form of the downfolded Hamiltonian is obtained as a consequence of utilizing active-space-dependent DUCC representation of the wave function

$$|\Psi\rangle = e^{\sigma_{\rm ext}} e^{\sigma_{\rm int}} |\Phi\rangle, \tag{1}$$

where $\sigma_{\rm ext}$ and $\sigma_{\rm int}$, referred to as external and internal cluster operators, are general-type anti-Hermitian operators[41] (see also Ref. 57),

$$\sigma_{\rm int}^{\dagger} = -\sigma_{\rm int}, \tag{2}$$

$$\sigma_{\rm ext}^{\dagger} = -\sigma_{\rm ext}. \tag{3}$$

The exactness of the expansion (1) is contingent upon the convergence of the infinite series, resulting in the multiple-step utilization of the Baker–Campbell–Hausdorff formula.[33] We will assume that these expansions are convergent. In analogy to the non-Hermitian case, the $\sigma_{\rm ext}$ and $\sigma_{\rm int}$ operators are defined by parameters [see Eqs. (30), (32), and (35) of Ref. 33] carrying only active spin-orbital labels and those with at least one in-active spin-orbital label, respectively. The DUCC ansatz employs analogous type of the cluster operator partitioning as discussed in the active-space[58–60] and tailored CC formulations.[61,62]

The use of the DUCC ansatz (1), in analogy to the SES-CC case, leads to an alternative way of determining energy, which can be obtained by solving the active-space Hermitian eigenvalue problem,

$$H^{\rm eff} e^{\sigma_{\rm int}} |\Phi\rangle = E e^{\sigma_{\rm int}} |\Phi\rangle, \tag{4}$$

where

$$H^{\rm eff} = (P + Q_{\rm int}) \bar{H}_{\rm ext} (P + Q_{\rm int}) \tag{5}$$

and

$$\bar{H}_{\rm ext} = e^{-\sigma_{\rm ext}} H e^{\sigma_{\rm ext}}. \tag{6}$$

The $Q_{\rm int}$ operator is a projection onto excited (with respect to $|\Phi\rangle$) configurations in complete active space (CAS), and the projection onto the reference function is denoted as P. When the external cluster amplitudes are known (or can be effectively approximated), the energy (or its approximation) can be calculated by diagonalizing the Hermitian effective/downfolded Hamiltonian (5) in the active space using various quantum or classical diagonalizers. It should also be stressed that for constructing effective Hamiltonians, only the $\sigma_{\rm ext}$ operator is needed ($\sigma_{\rm int}$ is only needed to represent its eigenvector). For well-defined active spaces [corresponding to small values of parameters defining $\sigma_{\rm ext}$ operators discussed in Eqs. (30) and (32) of Ref. 33], it is reasonable to assume that many-body series mentioned in the previous paragraph are convergent. The DUCC techniques provide a framework for a hierarchical structure of many-body approximations to construct effective Hamiltonians of increasing accuracies.

Although the DUCC downfolding procedure results in the effective Hamiltonians defined in active spaces, their properties differ from those of effective Hamiltonians used in the genuine multi-reference CC (MR-CC) approaches.[21,63–68] The main difference is a different, single-reference type characterization of the excitation manifold included in $\sigma_{\rm ext}$ compared to MR-CC methods. For example, typical manifestation of the intruder-state problem is associated with the appearance of excessively large MR-CC amplitudes defined by high-lying active and low-lying in-active spin-orbitals. These amplitudes are not present in the DUCC downfolding formalism. The proper choice of the active space provides large values of denominators in the perturbative analysis of $\sigma_{\rm ext}$ amplitudes. An additional factor in eliminating the intruder-state problem is the variational character of the ground-state eigenvalue of $H^{\rm eff}$ when an exact form of $e^{-\sigma_{\rm ext}} H e^{\sigma_{\rm ext}}$ can be determined.

For quantum computing applications, a second-quantized representation of $H^{\rm eff}$ is required. In the light of the non-commuting character of components defining the $\sigma_{\rm ext}$ operator, to this end, one has to rely on the finite-rank commutator expansions, i.e.,

$$\bar{H}_{\rm ext} \simeq H + \sum_{i=1}^{{\rm Max}_{\rm R}} \frac{1}{i!} [\ldots [H, \sigma_{\rm ext}], \ldots], \sigma_{\rm ext}]_i, \tag{7}$$

where $\mathrm{Max_R}$ stands for the length of commutator expansion. Due to the numerical costs associated with the contractions of multi-dimensional tensors, only approximations based on including low-rank commutators are feasible. In recent studies, approximations based on single, double, and part of triple commutators were explored, where one- and two-body interactions were retained in the second quantized form of H^{eff}. In practical applications, one also has to determine the approximate form of σ_{ext}. For practical reasons, we used the following approximation:

$$\sigma_{\mathrm{ext}} \simeq T_{\mathrm{ext}} - T_{\mathrm{ext}}^{\dagger}, \tag{8}$$

where T_{ext} can be defined through the external parts of the typical SR-CC cluster operators.

For further advancing of the CC downfolding techniques, two questions need to be addressed: (1) what is the impact of the choice of T_{ext} on the quality of ground-state energy of H^{eff}? and (2) what are the energy values corresponding to the untruncated (exact) form of H^{eff}? We answer these questions using the stringMB code that allows us to deal with the exact matrix representations of second quantized operators and their functions in the FCI space.

III. IMPLEMENTATION

For interacting fermionic systems, the action of the creation/annihilation operators for the electron in the pth spin-orbital ($a_p/a_p^{\dagger}$) on the Slater determinants can be conveniently described using the occupation number representation, where each Slater determinant is represented as a vector,

$$|n_M\ n_{M-1}\ \ldots\ n_{i+1}\ n_i\ n_{i-1}\ \ldots\ n_1\rangle, \tag{9}$$

where the occupation numbers n_i are equal to either 1 (electron occupies the ith spin orbital) or 0 (no electron is occupying the ith spin orbital) and M stands for the total number of spin-orbitals used to describe the quantum system and $M = 2N$, in which N is the number of orbitals.

The following formulas give the non-trivial action of creation/annihilation operators on the state vectors:

$$\begin{aligned} a_i^{\dagger}|n_M\ n_{M-1}\ \ldots\ n_{i+1}\ 0\ n_{i-1}\ \ldots n_1\rangle \\ = (-1)^{\sum_{k=1}^{i-1} n_k}|n_M\ n_{M-1}\ \ldots\ n_{i+1}\ 1\ n_{i-1}\ \ldots n_1\rangle, \end{aligned} \tag{10}$$

$$\begin{aligned} a_i|n_M\ n_{M-1}\ \ldots\ n_{i+1}\ 1\ n_{i-1}\ \ldots n_1\rangle \\ = (-1)^{\sum_{k=1}^{i-1} n_k}|n_M\ n_{M-1}\ \ldots\ n_{i+1}\ 0\ n_{i-1}\ \ldots n_1\rangle. \end{aligned} \tag{11}$$

Using the occupation-number representation, the stringMB code allows one to construct a matrix representation (A) of general second-quantized operators A, where A can be identified with electronic Hamiltonian, the external part of the cluster operator T_{ext}, and the exponents of $T_{\mathrm{ext}} - T_{\mathrm{ext}}^{\dagger}$, i.e.,

$$H \to \mathbf{H}, \tag{12}$$

$$T_{\mathrm{ext}} \to \mathbf{T}_{\mathrm{ext}}, \tag{13}$$

$$e^{\sigma_{\mathrm{ext}}} \simeq e^{T_{\mathrm{ext}} - T_{\mathrm{ext}}^{\dagger}} \to e^{\mathbf{T}_{\mathrm{ext}} - \mathbf{T}_{\mathrm{ext}}^{\dagger}}, \tag{14}$$

$$e^{-\sigma_{\mathrm{ext}}} \simeq e^{-(T_{\mathrm{ext}} - T_{\mathrm{ext}}^{\dagger})} \to e^{-(\mathbf{T}_{\mathrm{ext}} - \mathbf{T}_{\mathrm{ext}}^{\dagger})}, \tag{15}$$

$$\bar{H}_{\mathrm{ext}} \to \bar{\mathbf{H}}_{\mathrm{ext}}, \tag{16}$$

$$H^{\mathrm{eff}} \to \mathbf{H}^{\mathrm{eff}}. \tag{17}$$

Moreover, the stringMB can extract the sub-blocks of matrices or their products corresponding to arbitrary active space. This feature is used to form matrix representations of the effective Hamiltonians H^{eff}.

IV. RESULTS

Owing to the memory requirements (associated with the storage of matrix representations of the operator) of the stringMB code, we can deal with relatively small systems yet epitomizing situations encountered in the calculations for larger systems and processes. For this reason, we employed ubiquitous models corresponding to the linear chains of hydrogen atoms: H6 and H8 models. By varying the distance between neighboring hydrogens ($R_{\mathrm{H-H}}$), one can smoothly transition from the single-reference character of the ground-state wave function for smaller $R_{\mathrm{H-H}}$ distances (≃2.0 a.u. or less) to quasi-degenerate regime (2.75 and 3.00 a.u.)—a typical situation encountered in bond breaking/forming processes.

TABLE I. Comparison of energies (in Hartree) of the downfolded Hamiltonians for the linear H6 system in the STO-3G basis set based on various sources of the external amplitudes T_{ext} used to approximate the σ_{ext} operator ($\sigma_{\mathrm{ext}} \simeq T_{\mathrm{ext}} - T_{\mathrm{ext}}^{\dagger}$). All simulations used restricted Hartree–Fock molecular orbitals 2, 3 and 4, 5 as active occupied and virtual orbitals, respectively. In the linear chain of the H atoms, the geometry is defined by the distance between neighboring hydrogen atoms ($R_{\mathrm{H-H}}$) in a.u.

$R_{\mathrm{H-H}}$	FCI	SD	SDT	SDTQ	DUCC-SD	DUCC-SDT	DUCC-SDTQ
1.50	−3.199 566	−3.199 332	−3.199 601	−3.199 566	−3.199 324	−3.199 562	−3.199 566
1.75	−3.245 936	−3.245 603	−3.246 054	−3.245 936	−3.245 547	−3.245 923	−3.245 936
2.00	−3.217 699	−3.217 277	−3.218 047	−3.217 699	−3.217 040	−3.217 655	−3.217 697
2.25	−3.156 624	−3.156 266	−3.157 559	−3.156 621	−3.155 447	−3.156 484	−3.156 618
2.50	−3.085 398	−3.085 691	−3.087 713	−3.085 380	−3.083 217	−3.084 962	−3.085 374
2.75	−3.016 841	−3.019 512	−3.022 159	−3.016 770	−3.012 642	−3.015 537	−3.016 758
3.00	−2.957 646	−2.967 326	−2.969 163	−2.957 405	−2.948 732	−2.953 850	−2.957 384

TABLE II. Comparison of energies (in Hartree) of the downfolded Hamiltonians for the linear H8 system in the STO-3G basis set based on various sources of the external amplitudes T_{ext} used to approximate the σ_{ext} operator ($\sigma_{ext} \simeq T_{ext} - T_{ext}^{\dagger}$). All simulations used restricted Hartree–Fock molecular orbitals 3, 4 and 5, 6 as active occupied and virtual orbitals, respectively. In the linear chain of the H atoms, the geometry is defined by the distance between neighboring hydrogen atoms (R_{H-H}) in a.u.

R_{H-H}	FCI	SD	SDT	SDTQ	DUCC-SD	DUCC-SDT	DUCC-SDTQ
1.50	−4.235 775	−4.235 111	−4.235 846	−4.235 775	−4.235 071	−4.235 757	−4.235 774
1.75	−4.315 273	−4.314 347	−4.315 504	−4.315 273	−4.314 173	−4.315 222	−4.315 271
2.00	−4.286 011	−4.284 844	−4.286 688	−4.286 013	−4.284 235	−4.285 862	−4.286 005
2.25	−4.208 339	−4.207 232	−4.210 169	−4.208 337	−4.205 334	−4.207 876	−4.208 316
2.50	−4.114 829	−4.115 000	−4.119 502	−4.114 795	−4.109 473	−4.113 350	−4.114 739
2.75	−4.023 783	−4.029 321	−4.035 510	−4.023 578	−4.013 082	−4.018 712	−4.023 447
3.00	−3.944 748	−3.972 672	−3.978 401	−3.943 920	−3.912 005	−3.921 323	−3.943 614

TABLE III. The DUCC-CCSDTQ results (in Hartree) for the H8 model (R_{H-H} = 2.0 a.u.) were obtained with the STO-3G basis set for various choices of active spaces.

FCI	DUCC-CCSDTQ ($\{\{3,4,5,6\}\}$)	DUCC-CCSDTQ ($\{\{2,3,6,7\}\}$)	DUCC-CCSDTQ ($\{\{1,2,7,8\}\}$)
−4.286 011	−4.286 005	−4.285 865	−4.285 853

TABLE IV. The DUCC-CCSDTQ results (in Hartree) were obtained for various geometries of the H8 model in the STO-3G basis set for the $\{2,3,4,5,6,7\}$-generated active space (see the text for details). In the linear chain of the H atoms, the geometry is defined by the distance between neighboring hydrogen atoms (R_{H-H}) in a.u.

R_{H-H}	FCI	CCSDTQ	DUCC-CCSDTQ
2.00	−4.286 011	−4.286 013	−4.286 008
2.50	−4.114 829	−4.114 795	−4.114 782
3.00	−3.944 748	−3.943 920	−3.944 137

These benchmark systems are commonly used to assess the accuracy of *ab initio* methodologies in dealing with strong correlation effects. We employed the STO-3G basis set[69] in all calculations and restricted Hartree–Fock (RHF) molecular bases composed of 6 and 8 molecular orbitals for H6 and H8 systems, respectively. The systems of linear chains of hydrogen atoms allow for the evaluation of the downfolding procedure for the most extreme conditions; while most chemical systems have apparent subspaces containing the most important correlation effects, the strong correlation regime in the H6 and H8 systems (R_{H-H} = 3.0 a.u.) has no obvious choice of the active space for the ground-state problem. According to the wave function analysis for large separations, all orbitals fall into the category of "important" or "active" orbitals, and, therefore, the role that the choice of SR-CC amplitudes plays in parameterizing σ_{ext} is amplified. The results of our simulations for H6 and H8 systems are summarized in Tables I–VI.

In Table I, we collected CC and DUCC results obtained for active space defined by two highest occupied orbitals (orbitals 2 and 3) and two lowest virtual orbitals (orbitals 4 and 5) (we will invoke $\{2,3,4,5\}$ active space naming convention). The canonical

TABLE V. Comparison of the CASSCF(4,4), active-space FCI, DUCC-CCSDTQ, and PDS(3)/PDS(4) energies for H6 and H8 model systems. The PDS(3)/PDS(4) approaches were applied to evaluate the ground-state energy of the DUCC-CCSDTQ effective Hamiltonians. The $\{2,3,4,5\}$- and $\{4,5,6,7\}$-generated active spaces were used for H6 and H8 systems, respectively.

Method	H6 (R_{H-H} = 2.0 a.u.)	H6 (R_{H-H} = 3.0 a.u.)	H8 (R_{H-H} = 2.0 a.u.)	H8 (R_{H-H} = 3.0 a.u.)
HF	−3.105 850	−2.675 432	−4.138 199	−3.572 347
CASSCF(4,4)	−3.175 370	−2.856 832	−4.205 528	−3.699 677
Active-space FCI	−3.166 938	−2.802 092	−4.190 602	−3.665 605
FCI	−3.217 699	−2.957 646	−4.286 011	−3.944 748
DUCC-CCSDTQ	−3.217 697	−2.957 384	−4.286 005	−3.943 614
PDS(3)	−3.214 888	−2.953 067	−4.283 332	−3.941 223
PDS(4)	−3.217 234	−2.956 712	−4.285 622	−3.943 349

TABLE VI. Comparison of energies obtained with finite commutator expansion (CCSDTQ based) for the downfolded Hamiltonians and exact downfolding (DUCC-CCSDTQ) for H6 and H8 models in the STO-3G basis set.

Max_R/method	H6 (R_{H-H} = 2.0 a.u.)	H6 (R_{H-H} = 3.0 a.u.)	H8 (R_{H-H} = 2.0 a.u.)	H8 (R_{H-H} = 3.0 a.u.)
$Max_R = 0$	−3.166 938	−2.802 092	−4.190 602	−3.665 605
$Max_R = 1$	−3.269 110	−3.116 145	−4.382 423	−4.228 605
$Max_R = 2$	−3.218 732	−2.976 207	−4.288 761	−3.986 313
$Max_R = 3$	−3.217 344	−2.949 796	−4.285 044	−3.927 241
$Max_R = 4$	−3.217 693	−2.956 814	−4.285 985	−3.941 744
$Max_R = 5$	−3.217 699	−2.957 632	−4.286 012	−3.944 383
$Max_R = 10$	3.217 697	−2.957 384	−4.286 005	−3.943 615
DUCC-CCSDTQ	−3.217 697	−2.957 384	−4.286 005	−3.943 614
FCI	−3.217 699	−2.957 646	−4.286 011	−3.944 748

CCSD, CCSDT, and CCSDTQ energies (the corresponding columns are denoted as SD, SDT, and SDTQ) are compared to the FCI ones and lowest eigenvalues of the downfolded Hamiltonian in the active space for CCSD (DUCC-SD), CCSDT (DUCC-SDT), and CCSDTQ (DUCC-SDTQ) sources of the external amplitudes T_{ext} to calculate $\sigma_{ext}(\hbar)$ according to formula (8). In the weakly correlated regimes, the external amplitudes are well described at all levels of SR-CC methods, so any choice of SR-CC amplitudes well parameterizes σ_{ext}, resulting in comparable accuracy with respect to the FCI energies. However, for larger R_{H-H} distances, the quality of T_{ext} matters. For example, for larger distances, only T_{ext} defined at the CCSDTQ level yields DUCC-SDTQ energies of the CCSDTQ/FCI quality for all geometries. Other approaches, CCSD and CCSDT, for larger values of R_{H-H}, provide energies significantly below the FCI ones. However, it is interesting to notice that the corresponding eigenvalues of DUCC-SD and DUCC-SDT can reinstate the variational character of ground-state energy despite using T_{ext} stemming from CCSD and CCSDT calculations, which is an important property of the DUCC approach.

The CC and DUCC results for various geometries of the H8 system are collected in Table II. In this case, we also used active spaces defined by the two highest occupied orbitals (orbitals 3 and 4) and the two lowest virtual orbitals (orbitals 5 and 6). For the equilibrium geometry, including the triple and quadruple excitations in the external cluster operator, results in the near-FCI quality of the DUCC results. The accuracy of the DUCC-SD formalism is also satisfactory (less than 0.7 milliHartree error with respect to the FCI result), showing the effectiveness of the DUCC formalism in compressing the dynamical correlation effects even in the case when a simple form of external amplitudes is invoked. In analogy to the H6 case, one can observe the variational breakdown of the CCSD and CCSDT results for the larger H–H separations and restoration of the variational character by the corresponding DUCC formulations.

The DUCC case of downfolding, based on approximate σ_{ext} operators, as in the case when parameterized with SR-CC amplitudes, is active-space specific (the so-called cluster amplitudes' universal problem discussed in Ref. 47). However, to explore to what extent the DUCC downfolding formalism depends on the active space definition, in Table III, we collected DUCC-CCSDTQ energies for the H8 model with R_{H-H} = 2.0 a.u. and three model spaces defined by the $\{3,4,5,6\}$, $\{2,3,6,7\}$, and $\{1,2,7,8\}$ orbitals. One can see that although the DUCC-CCSDTQ energies are not equal, the energy discrepancies between results corresponding to various active spaces do not exceed 0.16 milliHartree.

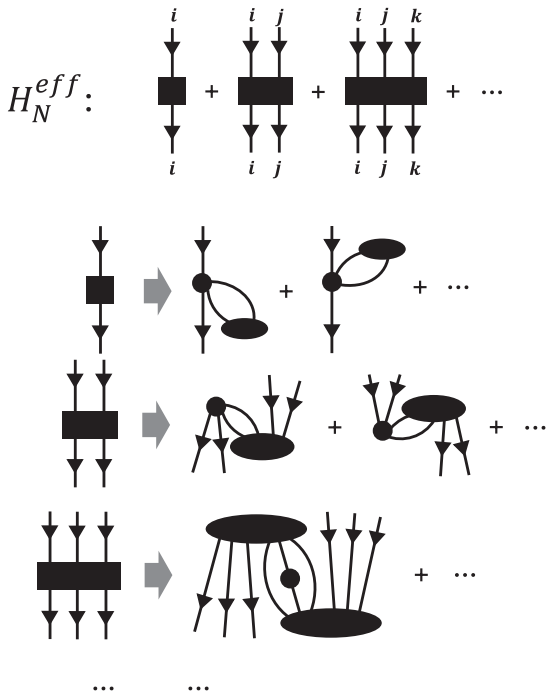

FIG. 1. Schematic representation of the many-body structure of the effective Hamiltonian in the normal product form (with respect to the reference function) defined for the smallest possible active space spanned by a single Slater determinant corresponding to the reference function $|\Phi\rangle$. The spin-orbital indices $i, j, k, \ldots$ refer to spin-orbitals occupied in $|\Phi\rangle$. The black rectangles and ovals refer to the Hugenholtz diagrammatic representation of anti-symmetrized effective interaction and cluster amplitude vertices, respectively.

The effect of the size of the active space is discussed in Table IV, where we collated the DUCC-CCSDTQ results obtained for various geometries of H8 and large $\{2,3,4,5,6,7\}$-generated active space. As expected, the increase in the active space size results in more accurate DUCC-CCSDT energies, especially for large distances. As discussed in Ref. 70, a powerful aspect of downfolded Hamiltonians is that the reduced dimensionality allows for higher-order description (excitations) to be included in the presence of external correlations through the effective Hamiltonian. This is demonstrated as the DUCC-CCSDTQ results surpass the CCSDTQ accuracy for $R_{\mathrm{H-H}} = 3.0$ a.u. due to the fact that higher-than-quadruple excitations are included in the diagonalization of the downfolded Hamiltonian in the active space.

The simplest active space that can be used by the DUCC formalism is defined by a reference function $|\Phi\rangle$, i.e., when all occupied spin-orbitals are considered active and when there are no active virtual orbitals. All correlation effects are compressed to the reference-occupied orbitals and encapsulated in interactions between electrons in the reference function. In this case, all operator expressions contributing to H^{eff} (or its normal product form H_N^{eff}; $H_N^{\mathrm{eff}} = H^{\mathrm{eff}} - \langle\Phi|H^{\mathrm{eff}}|\Phi\rangle$) can be represented as the product of the particle number operators, $n_p = a_p^\dagger a_p$, for p's corresponding to occupied spin-orbital indices denoted as $i, j, k, \ldots$ (see Fig. 1), i.e.,

$$\prod_{\alpha} n_{i(\alpha)}. \tag{18}$$

The DUCC-CCSD and DUCC-CCSDTQ energies for this case are shown in Fig. 2 and compared with CCSD, CCSDTQ, and FCI ones. As seen from Fig. 2 (top panel), each DUCC formalism defines effective interactions correlating electrons in occupied spin-orbitals that significantly improve the quality of the RHF model. The DUCC-CCSD errors with respect to the FCI energies for $R_{\mathrm{H-H}} = 2.0$ a.u. and $R_{\mathrm{H-H}} = 3.0$ a.u. amount to 0.92 and 20.52 milliHartree, respectively, whereas analogous errors for the DUCC-CCSDTQ are equal to 0.08 and 3.70 milliHartree, respectively. These errors should be compared to RHF energy errors of 118.85 and 282.21 milliHartree.

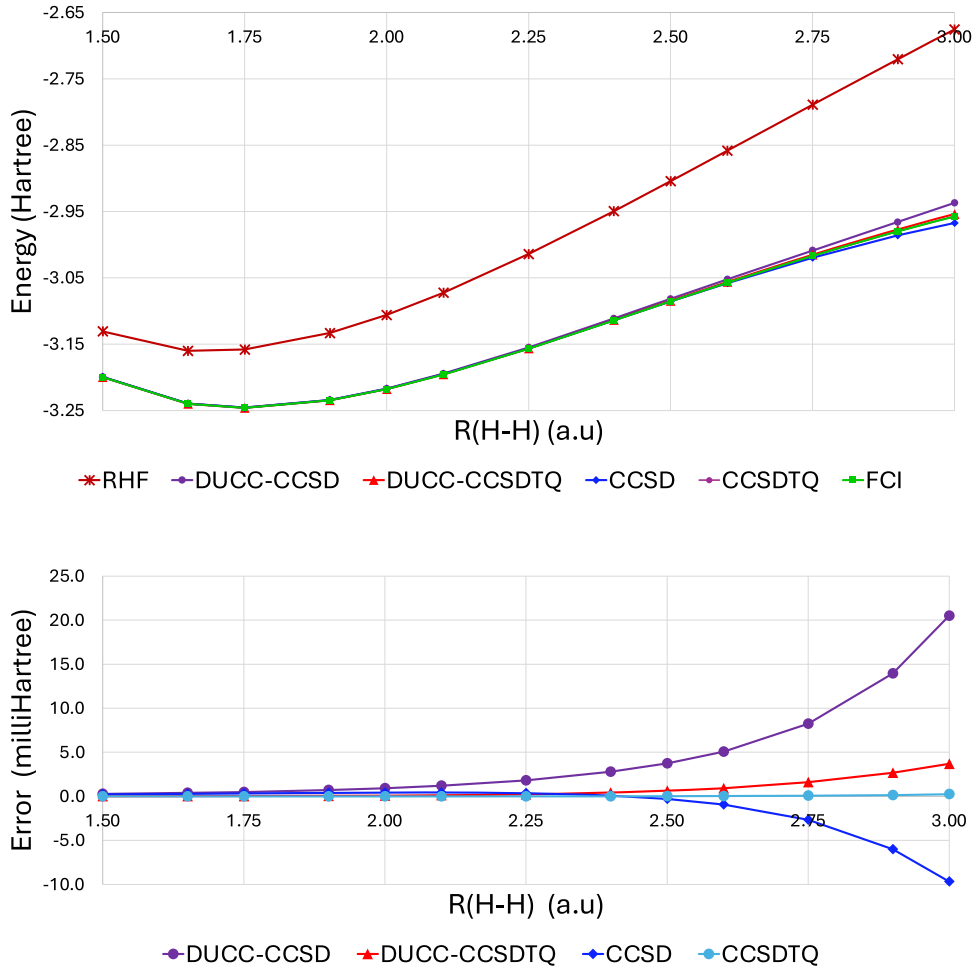

FIG. 2. Comparison of ground-state energies [reported as total energies (top panel) and errors (bottom panel) with respect to the FCI results] obtained with the DUCC, CC, and FCI methods for the smallest active space defined by the reference function $|\Phi\rangle$ of the H6 model system in the STO-3G basis set.

From the point of view of quantum computing application, it is essential to evaluate the performance of techniques to approximate the many-body forms of the downfolded Hamiltonians and the potential accuracies of quantum solvers. To this end, we will analyze the finite rank expansion for Eq. (7) and the variant of the Connected Methods Expansion (CMX)[71–76] based on the Peeters–Devreese–Soldatov (PDS) functional,[77,78] which has been recently explored in the context of quantum computing.[79–81] In this paper, we will apply low-rank PDS formulations PDS(3) and PDS(4) (for details, we refer the reader to Refs. 77 and 78) to identify ground-state energies of the downfolded Hamiltonians. It is worth noting that the low ranks of the PDS approach can be effectively implemented on quantum computers. The PDS results are collated in Table V, providing Hartree–Fock, complete active space self-consistent field (using four active electrons distributed over four active orbitals), and active-space FCI energies. For H6 and H8 models, we used $\{2,3,4,5\}$- and $\{4,5,6,7\}$-generated active spaces, respectively. Before discussing the PDS results, we should stress the efficiency of the downfolding procedures (here illustrated in the example of the DUCC-CCSDTQ approach) in capturing the out-of-active-space correlation effect. This is best illustrated by comparing DUCC-CCSDTQ vs CASSCF(4,4) and active-space FCI energies. Despite using the same active space definitions, the CASSCF(4,4) and active-space FCI energies for all geometries of H6 and H8, in contrast to the DUCC-CCSDTQ approach, are characterized by significant errors with respect to the FCI energies. Although, in many cases, quantum simulations are performed for small dimensionality active spaces using bare Hamiltonians, the quality of the results can be significantly improved without a significant increase in quantum computing resources by using a downfolded form of the Hamiltonian. As seen from Table V, the PDS(3) can provide much better quality results than active-space FCI. The PDS(4) can further refine the accuracies of the PDS(3) approach, reducing the errors with respect to exact DUCC-CCSDTQ energies to within 0.7 milliHartree for H6 and H8 model systems. In the last part of our discussion, we analyze the accuracies of the finite rank (Max_R) approximations for downfolded Hamiltonians. The results for H6 and H8 models are collected in Table VI. The convergence of the commutator expansions is illustrated in the example of the tenth-rank commutator expansion. In all cases discussed in Table VI, $\mathrm{Max}_R = 10$ approximation reproduces virtually the exact DUCC-CCSDTQ energies. In practical applications based on the many-body form of the downfolded Hamiltonian, only low-rank commutator expansions ($\mathrm{Max}_R = 1, \ldots, 4$) are numerically feasible (the $\mathrm{Max}_R = 0$ corresponds to the active-space FCI results). One can observe that for weakly correlated situations ($R_{\mathrm{H-H}} = 2.0$ a.u.), $\mathrm{Max}_R = 3$ provides a satisfactory approximation of the exact DUCC-CCSDTQ energies. For a strongly correlated case ($R_{\mathrm{H-H}} = 3.0$ a.u.), the inclusion of the fourth rank commutators ($\mathrm{Max}_R = 4$) is needed. In practical applications, however, all expansions are based on the mixing of $\mathrm{Max}_R = n$ contributions with $n + 1$-rank commutators stemming from the Fock matrix terms to reinstate the so-called perturbative balance (see Ref. 70 for the discussion). For example, $\mathrm{Max}_R = 1$ case epitomizes a situation where the perturbative balance is violated, and non-variational energies can be obtained. Therefore, for the strongly correlated cases, we recommend the expansions based on the inclusion of $\mathrm{Max}_R = 3$ or $\mathrm{Max}_R = 4$ terms with the Fock-operator-dependent terms originating in the fourth and fifth commutators, respectively. While the STO-3G basis set helps validate the downfolding procedures, more extensive basis sets that adequately capture short-range dynamical correlation effects are required in realistic applications. To address this challenge, we have implemented a two-step strategy, referred to as the DUCC-SD(solver) procedure, which utilizes two steps: (1) CC active space downfolding and (2) solving downfolded Hamiltonians using the CCSD approach. We employ this procedure to H8 in the cc-pVDZ basis set (including 40 orbitals) and active spaces defined by the 9 lowest RHF orbitals. Due to the size of the FCI problem in the cc-pVDZ basis set, we use the approximate form of downfolding defined by the commutator expansion that includes single and double commutators and part of triple commutator defined by the Fock operator (as defined in Ref. 70). The external cluster operator σ_{ext} is approximated by $T_{\mathrm{ext}} - T_{\mathrm{ext}}^{\dagger}$, where T_{ext} is obtained in the CCSD calculations. In the effective Hamiltonian, we include one- and two-body interactions only. The results of cc-pVDZ simulations are shown in Table VII. The DUCC-SD(solver) results are in qualitative agreement with the CCSDTQ results for two geometries considered, where the absolute values of errors with respect to the CCSDTQ energies amount to 1.7 and 0.4 milliHartree for 2.0 and 3.0 a.u. geometries, respectively. This is in contrast to the 6.6 and 3.7 milliHartree errors of canonical CCSD. This DUCC-SD(solver) procedure efficiently captures the dynamical correlation of the cc-pVDZ basis while including important higher-order correlation effects, which are captured by the diagonalization of the effective Hamiltonians in the active space.

TABLE VII. Comparison of energies (in Hartree) obtained with various all-orbital CC approximations and the DUCC-SD(solver) procedure defined using the nine lowest-energy active orbitals for the H8 model in the cc-pVDZ basis set. The details of the DUCC-SD(solver) approach are described in Sec. IV. The distance between neighboring hydrogen atoms ($R_{\mathrm{H-H}}$) is defined in a.u.

$R_{\mathrm{H-H}}$	CCSD	CCSDT	CCSDTQ	DUCC-SD(solver)
2.00	−4.471 759	−4.476 680	−4.476 653	−4.478 331
3.00	−4.210 982	−4.220 303	−4.214 348	−4.214 710

V. CONCLUSION

A series of calculations were conducted to examine the impact of approximations on external cluster amplitudes on CC downfolded energies. Simple model systems, H6 and H8 linear chains, were utilized to continuously vary the extent of correlation effects from weakly to strongly correlated regimes (with $R_{\mathrm{H-H}}$ ranging from 2.0 to 3.0 a.u.). The results showed that while the external cluster amplitudes from SR-CCSD calculations were satisfactory for the weakly correlated situation, for the strongly correlated case, the effect of triply and quadruply excited external clusters could no longer be neglected. The downfolding procedure acted as a stabilizer and could restore the variational character of energies despite the fact that external amplitudes were obtained from SR-CC calculations that suffer from the variational collapse. Furthermore, the downfolded energies obtained for various active spaces on the H8 systems (including those that did not include essential correlation effects) had only small discrepancies, demonstrating the approximate invariance of downfolding energies for various active spaces.

This was the case for all SES-CC types of active spaces for commutative SR-CC formulations. In addition, it was shown that the downfolded Hamiltonians could be effectively diagonalized with low-order PDS formulations for both weakly and strongly correlated regimes.

The assessment of the impact of the maximum rank of the commutator expansion on the precision of downfolded energies is an integral aspect of the analysis associated with practical applications of CC downfolding procedures. Our findings demonstrate that an increase in the degree of correlation effects necessitates the inclusion of higher rank commutators. In particular, for H6/H8 R_{H-H} = 2.0 a.u., the inclusion of single, double, and triple commutators is sufficient to achieve a favorable agreement with the FCI energies. However, for R_{H-H} = 3.0 a.u., higher-order commutators (quadruple/pentuple) must be incorporated into the approximation. It should be noted, however, that for the R_{H-H} = 3.0 a.u. scenario, an active space that can distinguish between static and dynamical correlation effects cannot be constructed (i.e., all orbitals must be considered active). Nonetheless, as Table VI demonstrates, the corresponding commutator-rank expansion rapidly converges to the FCI energies.

The results of downfolding for the smallest active space defined by a single Hartree–Fock determinant are auspicious. Although this model generally involves higher-rank interactions (e.g., three- and higher many-body interactions), it is possible to utilize the downfolding procedure to achieve high-accuracy energies by correlating electrons in the occupied spin-orbitals only. Furthermore, in this case, all second quantized operators can be represented as products of particle number operators corresponding to occupied spin-orbitals. This approach can also guide machine learning models in determining effective interactions in the occupied spin-orbital space.

ACKNOWLEDGMENTS

This work was supported by the "Transferring exascale computational chemistry to cloud computing environment and emerging hardware technologies (TEC^4)" project, which is funded by the U.S. Department of Energy, Office of Science, Office of Basic Energy Sciences, the Division of Chemical Sciences, Geosciences, and Biosciences (under Grant No. FWP 82037). This work used resources from the Pacific Northwest National Laboratory (PNNL). PNNL is operated by Battelle for the U.S. Department of Energy under Contract No. DE-AC05-76RL01830.

AUTHOR DECLARATIONS

Conflict of Interest

The authors have no conflicts to disclose.

Author Contributions

Karol Kowalski: Conceptualization (equal); Methodology (equal); Software (equal); Writing – original draft (equal); Writing – review & editing (equal). **Bo Peng**: Conceptualization (equal); Writing – original draft (equal); Writing – review & editing (equal). **Nicholas P. Bauman**: Conceptualization (equal); Methodology (equal); Writing – original draft (equal); Writing – review & editing (equal).

DATA AVAILABILITY

The data that support the findings of this study are available from the corresponding author upon reasonable request.

REFERENCES

[1] T. Takeshita, N. C. Rubin, Z. Jiang, E. Lee, R. Babbush, and J. R. McClean, Phys. Rev. X **10**, 011004 (2020).
[2] B. Şahinoğlu and R. D. Somma, npj Quantum Inf. **7**, 119 (2021).
[3] J. Liu, Z. Li, and J. Yang, J. Chem. Theory Comput. **18**, 4795 (2022).
[4] R. Huang, C. Li, and F. A. Evangelista, PRX Quantum **4**, 020313 (2023).
[5] A. Peruzzo, J. McClean, P. Shadbolt, M.-H. Yung, X.-Q. Zhou, P. J. Love, A. Aspuru-Guzik, and J. L. O'brien, Nat. Commun. **5**, 4213 (2014).
[6] J. R. McClean, J. Romero, R. Babbush, and A. Aspuru-Guzik, New J. Phys. **18**, 023023 (2016).
[7] J. Romero, R. Babbush, J. R. McClean, C. Hempel, P. J. Love, and A. Aspuru-Guzik, Quantum Sci. Technol. **4**, 014008 (2018).
[8] A. Kandala, A. Mezzacapo, K. Temme, M. Takita, M. Brink, J. M. Chow, and J. M. Gambetta, Nature **549**, 242 (2017).
[9] A. Kandala, K. Temme, A. D. Córcoles, A. Mezzacapo, J. M. Chow, and J. M. Gambetta, Nature **567**, 491 (2019).
[10] A. F. Izmaylov, T.-C. Yen, R. A. Lang, and V. Verteletskyi, J. Chem. Theory Comput. **16**, 190 (2019).
[11] R. A. Lang, I. G. Ryabinkin, and A. F. Izmaylov, J. Chem. Theory Comput. **17**, 66 (2021).
[12] H. R. Grimsley, S. E. Economou, E. Barnes, and N. J. Mayhall, Nat. Commun. **10**, 3007 (2019).
[13] H. R. Grimsley, D. Claudino, S. E. Economou, E. Barnes, and N. J. Mayhall, J. Chem. Theory Comput. **16**, 1 (2019).
[14] S. McArdle, S. Endo, A. Aspuru-Guzik, S. C. Benjamin, and X. Yuan, Rev. Mod. Phys. **92**, 015003 (2020).
[15] W. M. Kirby and P. J. Love, Phys. Rev. Lett. **127**, 110503 (2021).
[16] J. Tilly, H. Chen, S. Cao, D. Picozzi, K. Setia, Y. Li, E. Grant, L. Wossnig, I. Rungger, G. H. Booth, and J. Tennyson, Phys. Rep. **986**, 1 (2022).
[17] F. Coester, Nucl. Phys. **7**, 421 (1958).
[18] F. Coester and H. Kummel, Nucl. Phys. **17**, 477 (1960).
[19] J. Čížek, J. Chem. Phys. **45**, 4256 (1966).
[20] J. Paldus, J. Čížek, and I. Shavitt, Phys. Rev. A **5**, 50 (1972).
[21] D. Mukherjee, R. K. Moitra, and A. Mukhopadhyay, Mol. Phys. **30**, 1861 (1975).
[22] B. Adams, K. Jankowski, and J. Paldus, Chem. Phys. Lett. **67**, 144 (1979).
[23] G. D. Purvis and R. J. Bartlett, J. Chem. Phys. **76**, 1910 (1982).
[24] B. Jeziorski and H. J. Monkhorst, Phys. Rev. A **24**, 1668 (1981).
[25] D. I. Lyakh, M. Musiał, V. F. Lotrich, and R. J. Bartlett, Chem. Rev. **112**, 182 (2012).
[26] G. Carleo and M. Troyer, Science **355**, 602 (2017).
[27] H. Wang, L. Zhang, J. Han, and E. Weinan, Comput. Phys. Commun. **228**, 178 (2018).
[28] D. Pfau, J. S. Spencer, A. G. Matthews, and W. M. C. Foulkes, Phys. Rev. Res. **2**, 033429 (2020).
[29] J. Hermann, Z. Schätzle, and F. Noé, Nat. Chem. **12**, 891 (2020).
[30] A. Anshu, S. Arunachalam, T. Kuwahara, and M. Soleimanifar, Nat. Phys. **17**, 931 (2021).
[31] S. Chen, Nat. Phys. **20**, 1745 (2024).
[32] N. P. Bauman and K. Kowalski, Mater. Theory **6**, 17 (2022).
[33] K. Kowalski and N. P. Bauman, J. Chem. Phys. **152**, 244127 (2020).
[34] N. P. Bauman, E. J. Bylaska, S. Krishnamoorthy, G. H. Low, N. Wiebe, C. E. Granade, M. Roetteler, M. Troyer, and K. Kowalski, J. Chem. Phys. **151**, 014107 (2019).

[35] H. Primas, Rev. Mod. Phys. **35**, 710 (1963).
[36] M. D. Prasad, S. Pal, and D. Mukherjee, Phys. Rev. A **31**, 1287 (1985).
[37] M. R. Hoffmann and J. Simons, J. Chem. Phys. **88**, 993 (1988).
[38] W. Kutzelnigg, Theor. Chim. Acta **80**, 349 (1991).
[39] R. J. Bartlett, S. A. Kucharski, and J. Noga, Chem. Phys. Lett. **155**, 133 (1989).
[40] A. G. Taube and R. J. Bartlett, Int. J. Quantum Chem. **106**, 3393 (2006).
[41] J. Lee, W. J. Huggins, M. Head-Gordon, and K. B. Whaley, J. Chem. Theory Comput. **15**, 311 (2018).
[42] T. Yanai and G. K. Chan, J. Chem. Phys. **124**, 194106 (2006).
[43] F. A. Evangelista and J. Gauss, J. Chem. Phys. **134**, 114102 (2011).
[44] F. A. Evangelista, G. K.-L. Chan, and G. E. Scuseria, J. Chem. Phys. **151**, 244112 (2019).
[45] N. H. Stair and F. A. Evangelista, PRX Quantum **2**, 030301 (2021).
[46] K. Kowalski, J. Chem. Phys. **148**, 094104 (2018).
[47] K. Kowalski, Phys. Rev. A **104**, 032804 (2021).
[48] K. Kowalski, J. Chem. Phys. **158**, 054101 (2023).
[49] N. He, C. Li, and F. A. Evangelista, J. Chem. Theory Comput. **18**, 1527 (2022).
[50] K. Kowalski and N. P. Bauman, Phys. Rev. Lett. **131**, 200601 (2023).
[51] G. E. Scuseria and H. F. Schaefer, Chem. Phys. Lett. **152**, 382 (1988).
[52] J. Noga and R. J. Bartlett, J. Chem. Phys. **86**, 7041 (1987).
[53] J. Noga and R. J. Bartlett, J. Chem. Phys. **89**, 3401 (1988).
[54] N. Oliphant and L. Adamowicz, J. Chem. Phys. **95**, 6645 (1991).
[55] P. Piecuch and L. Adamowicz, J. Chem. Phys. **100**, 5792 (1994).
[56] S. A. Kucharski and R. J. Bartlett, Theor. Chim. Acta **80**, 387 (1991).
[57] P. Piecuch, K. Kowalski, P.-D. Fan, and K. Jedziniak, Phys. Rev. Lett. **90**, 113001 (2003).
[58] N. Oliphant and L. Adamowicz, J. Chem. Phys. **94**, 1229 (1991).
[59] N. Oliphant and L. Adamowicz, J. Chem. Phys. **96**, 3739 (1992).
[60] P. Piecuch, N. Oliphant, and L. Adamowicz, J. Chem. Phys. **99**, 1875 (1993).
[61] T. Kinoshita, O. Hino, and R. J. Bartlett, J. Chem. Phys. **123**, 074106 (2005).
[62] M. Ravi, A. Perera, Y. C. Park, and R. J. Bartlett, J. Chem. Phys. **159**, 094101 (2023).
[63] B. Jeziorski and H. J. Monkhorst, Phys. Rev. A **24**, 1668 (1981).
[64] B. Jeziorski and J. Paldus, J. Chem. Phys. **90**, 2714 (1989).
[65] L. Meissner and R. J. Bartlett, J. Chem. Phys. **92**, 561 (1990).
[66] L. Meissner, J. Chem. Phys. **108**, 9227 (1998).
[67] J. Paldus, P. Piecuch, L. Pylypow, and B. Jeziorski, Phys. Rev. A **47**, 2738 (1993).
[68] K. Kowalski and P. Piecuch, Phys. Rev. A **61**, 052506 (2000).
[69] W. J. Hehre, R. F. Stewart, and J. A. Pople, J. Chem. Phys. **51**, 2657 (1969).
[70] N. P. Bauman and K. Kowalski, J. Chem. Phys. **156**, 094106 (2022).
[71] D. Horn and M. Weinstein, Phys. Rev. D **30**, 1256 (1984).
[72] J. Cioslowski, Phys. Rev. Lett. **58**, 83 (1987).
[73] P. J. Knowles, Chem. Phys. Lett. **134**, 512 (1987).
[74] J. D. Mancini, Y. Zhou, and P. F. Meier, Int. J. Quantum Chem. **50**, 101 (1994).
[75] J. Noga, A. Szabados, and P. R. Surján, Int. J. Mol. Sci. **3**, 508 (2002).
[76] B. Ganoe and M. Head-Gordon, J. Chem. Theory Comput. **19**, 9187 (2023).
[77] F. Peeters and J. Devreese, J. Phys. A: Math. Gen. **17**, 625 (1984).
[78] A. Soldatov, Int. J. Mod. Phys. B **09**, 2899 (1995).
[79] K. Kowalski and B. Peng, J. Chem. Phys. **153**, 201102 (2020).
[80] B. Peng and K. Kowalski, Quantum **5**, 473 (2021).
[81] D. Claudino, B. Peng, N. P. Bauman, K. Kowalski, and T. S. Humble, Quantum Sci. Technol. **6**, 034012 (2021).